ADVANCED FUNCTIONAL MATERIALS
www.afm-journal.de

Materials Views
www.MaterialsViews.com

Efficient Persistent Room Temperature Phosphorescence in Organic Amorphous Materials under Ambient Conditions

Shuzo Hirata, Kenro Totani, Junxiang Zhang, Takashi Yamashita, Hironori Kaji, Seth R. Marder, Toshiyuki Watanabe,* and Chihaya Adachi**

Persistent emission with a long lifetime (>1 s) from organic materials can only be observed at a low temperature, because of the significant nonradiative deactivation pathway that occurs at room-temperature (RT). If organic materials with persistent RT emission in air could be developed, they could potentially be utilized for a variety of applications. Here, organic host-guest materials with efficient persistent RT phosphorescence (RTP) are developed by minimizing the nonradiative deactivation pathway of triplet excitons. The nonradiative deactivation pathway is dependent on both nonradiative deactivation of the guest and quenching by diffusional motion of the host. The rigidity and oxygen barrier properties of the steroidal compound used as the host suppressed the quenching, and the aromatic hydrocarbon used as the guest is highly deuterated to minimize nonradiative deactivation of the guest. Red-green-blue persistent RTP with a lifetime >1 s and a quantum yield >10% in air is realized for a pure organic material.

Prof. S. Hirata
Department of Polymer Science
and Organic Materials Engineering
Tokyo Institute of Technology
2-12-1, Meguro, Tokyo 152-8552, Japan
E-mail: hirata.s.af@m.titech.ac.jp
Dr. K. Totani, Prof. T. Watanabe
Division of Applied Chemistry
Graduate School of Engineering
Tokyo University of Agriculture and Technology
2-24-16 Naka, Koganei, Tokyo 184-8588, Japan
E-mail: toshi@cc.tuat.ac.jp
Dr. J. Zhang, Prof. S. R. Marder
Center for Organic Photonics and Electronics (COPE) and School of Chemistry and Biochemistry
Georgia Institute of Technology
901 Atlantic Drive, Atlanta, GA 30332-0400, USA
Prof. T. Yamashita
Pure and Applied Chemistry
Science and Technology
Tokyo University of Science
2641 Yamazaki, Noda, Chiba 278-8510, Japan
Prof. H. Kaji
Institute for Chemical Research
Kyoto University
Uji, Kyoto 611-0011, Japan
Prof. C. Adachi
Center for Organic Photonics and Electronics Research (OPERA)
Kyushu University
744 Motooka, Nishi, Fukuoka 819-0395, Japan
E-mail: adachi@cstf.kyushu-u.ac.jp

DOI: 10.1002/adfm.201203706

1. Introduction

Room temperature phosphorescence (RTP) could create new opportunities in the development of photodynamic therapy,[1–3] optical limiters,[4,5] organic light emitting diodes,[6–9] and bioimaging,[10,11] but RTP is typically a function of organometallic materials. Although efficient RTP from metal-free organic crystalline materials has been observed in air,[12,13] compatibility of specific molecular configuration and special intermolecular interactions between molecules is requisite for RTP function, which significantly limits applications and functionalization of the compounds due to their restricted sample shapes and chemical structural designs. If amorphous pure organic RTP materials could be obtained, the materials would have advantages such as a variety of functionalization due to an expansive chemical structural design, and free scalability of sample shape due to the amorphous state. Furthermore, it is well known that RTP from the organometallic[6–9] and metal-free[12,13] materials shows significantly short phosphorescence lifetime, which is typically shorter than 10 ms, and it exhibits no persistent emission. RTP with a persistent emission is attractive for truly high contrast imaging using inexpensive and small-scale photodetector, which is independent of the emissive noise of the background.[14,15] Contrary to inorganic materials with persistent RT emission,[14–17] the organic amorphous materials with persistent RTP are expansive to a variety of background-independent imaging applications, because the attachment of functional groups can create novel emitting probes. For example, the combinations between organic fluorescent compounds and other functional compounds have created new photoresponsive[18–20] and thermoresponsive[21–24] fluorescent probes for ultra-high density optical storage,[18,19,25] ultra-high resolution bioimaging,[19,25–27] and advanced security imaging.[20–24] Therefore, organic persistent RTP with the unique function is potentially utilized for a variety of imaging and display applications.

The key issue for pure organic amorphous materials with persistent RTP in air is control of the radiative and nonradiative decay rates of the lowest triplet excited state (T_1 state) at RT in air. This is particularly important because pure organic materials have small radiative decay rates ($<10^0$ s^{-1}), and it is critical to significantly suppress the nonradiative decay rate that

depopulates the T_1 state.[28] However, suppression of nonradiative and quenching processes of the T_1 state in conventional pure organic amorphous materials at RT are difficult to control, and RTP has not been observed from pure organic amorphous materials in air.

Here we present a systematic strategy to suppress the nonradiative deactivation pathways for long-lifetime RT triplet excitons and produce organic amorphous materials with efficient red-green-blue (RGB) persistent RTP in air. The concept involves the design of aromatic guests with no heavy atoms such as metals and halogens to minimize nonradiative deactivation, because the introduction of such atoms shortens the excited state lifetime so that radiative lifetimes longer than 1 s become unavailable. In addition, different from the crystalline textures reported in previous studies,[12,13] we propose the new idea of a guest-host system in which the aromatic guests are surrounded by a rigid amorphous host with short π conjugation. Such a host-guest amorphous film would successfully realize compatibility of a significantly long excited state lifetime and rather high photoluminescence (PL) efficiency from a variety of aromatic carbons.

Amorphous organic materials composed of a secondary amino-substituted deuterated carbon as the guest and a hydroxyl steroidal compound as the host matrix (**Figure 1**(i)) were prepared. The use of an amorphous rigid steroidal compound as a host significantly minimizes the quenching of long-lifetime RT triplet excitons of the guest by interaction with the host matrix and oxygen ($k_q(RT)$) (Figure 1(ii)). Appropriate structural design of the guest reduces the nonradiative decay rate constant of the guest at RT ($k_{nr}(RT)$) (Figure 1(iii)). This combination of guest and host leads to significantly small nonradiative processes at RT ($k_{nr}(RT)+k_q(RT)$) in air, which are smaller than the small radiative rate constant ($k_r<10^0$ s^{-1}) (Figure 1(iv)), resulting in efficient persistent RTP that remains in air after photoexcitation was stopped, as shown in Figure 1(v). **Figure 2** shows a demonstration of efficient persistent RTP under atmospheric conditions. The transparent sample film was a host-guest system composed of the appropriate designed guest (mass fraction 0.3%) and steroidal host matrix on a glass substrate. Efficient red persistent RTP was clearly observed from the pure organic host-guest film for several seconds after scanning with an excitation beam at 405 nm under atmospheric conditions. After the excitation beam has passed through the guest-host layer from the lower to the upper side (i), the trajectory of bright red persistent RTP remained for several seconds (ii) because the phosphorescence lifetime was longer than 1 s. Figures 2(iii,iv) show that the trajectory of red persistent RTP generated during the first scan of the excitation beam still remained after the second scan. Demonstrations of efficient persistent RTP in pure organic host-guest films showing other phosphorescence colors are shown in Supporting Information Movies S1 to S4. In addition to long RTP lifetimes (a few seconds), these materials have RTP quantum efficiencies of >10% for RGB RTP in air.

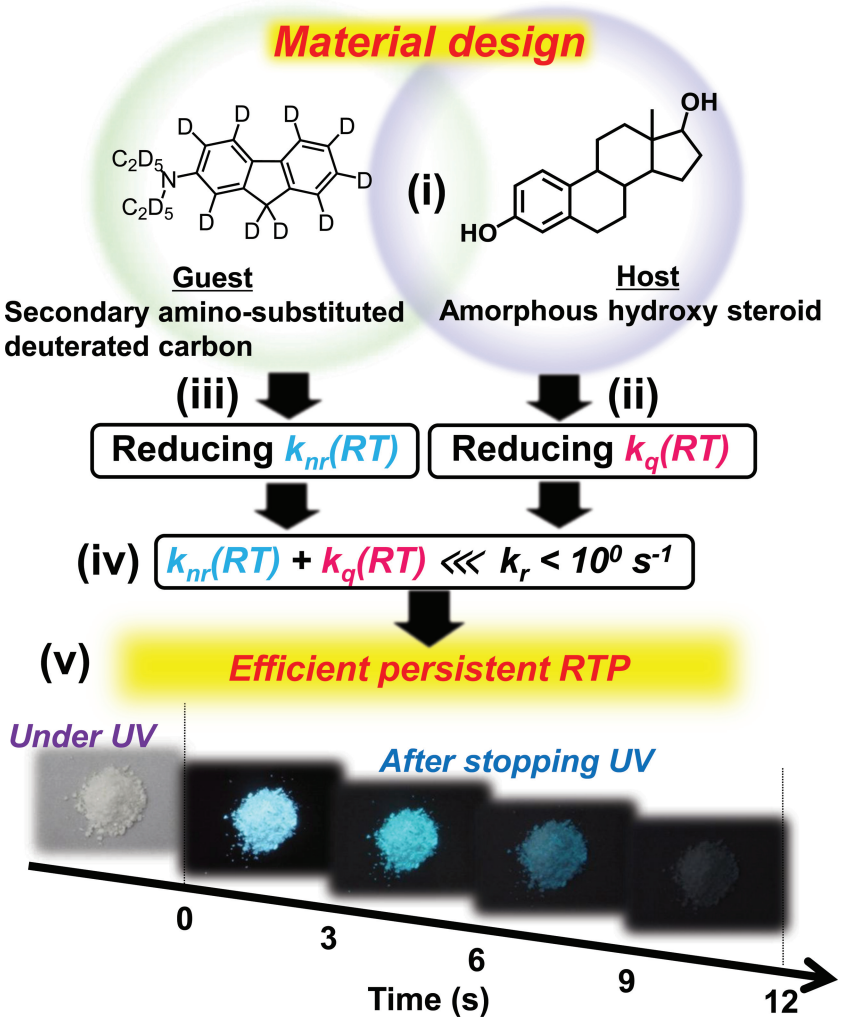

Figure 1. Material design for efficient persistent RTP in air. Organic amorphous materials with efficient persistent RTP in air were constructed using a secondary amino-substituted deuterated hydrocarbon as the guest and an amorphous hydroxy steroidal compound as the host (i). An amorphous rigid structure with a large energy gap, such as a hydroxy steroidal compound, minimizes quenching of the triplet excitons of the guest by interaction with the host matrix and oxygen ($k_q(T)$) (ii). Appropriate structural design of the guest, which is shown in Figure 7, reduces its nonradiative decay rate constant ($k_{nr}(RT)$) (iii). The combination of guest and host leads to a significant decrease of the nonradiative decay rate, resulting in $k_{nr}(RT)+k_q(RT)<<<k_r<10^0$ s^{-1} (iv). The significant decrease of the nonradiative decay rate provides efficient persistent RTP that remains in air after photoexcitation (v).

2. Appropriate Conditions for Efficient Persistent RTP

Appropriate compounds for efficient persistent RTP were investigated using various organic luminescent molecules

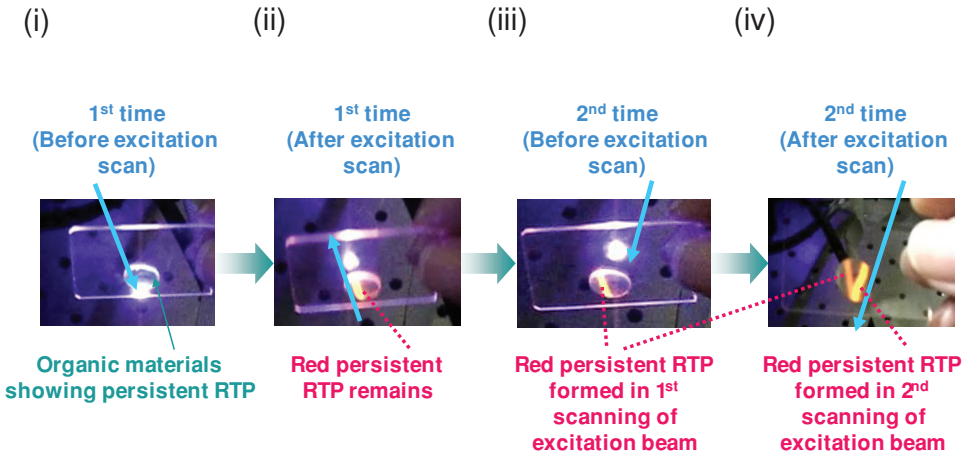

Figure 2. Demonstration of efficient persistent RTP from organic materials under atmospheric conditions. The sample film was a host-guest system composed of dye 19 (mass fraction 0.3%) as the guest and β-estradiol as the host matrix on a glass substrate.

as the guest and conventional vinyl polymers and steroidal compounds as the host matrix, as shown in **Figure 3**. The phosphorescence quantum yield at T [K] ($\Phi_P(T)$) and the phosphorescence lifetime at T [K] ($\tau(T)$) are expressed by Equations 1 and 2, respectively.

$$\phi_P(T) = \phi_{ISC}(T) k_r \tau(T) \quad (1)$$

$$\tau(T) = 1/(k_r + k_{nr}(T) + k_q(T)) \quad (2)$$

where $\Phi_{ISC}(T)$ is the quantum efficiency for intersystem crossing from the lowest singlet state (S_1 state) to the T_1 state at T [K], k_r is the rate constant for phosphorescence, $k_{nr}(T)$ is the rate constant for nonradiative deactivation from the T_1 state of a guest at T [K], and $k_q(T)$ is the rate constant based on quenching of the triplet exciton of a guest by interaction with the host matrix and oxygen at T [K]. Both $k_{nr}(T)$ and $k_q(T)$ are strongly dependent on temperature. Based on Equations 1 and 2, $k_{nr}(RT)$ and $k_q(RT)$ should be at least smaller than k_r ($<10^0$ s^{-1})[28] with large $\Phi_{ISC}(RT)$ to obtain efficient persistent RTP.

3. Result and Discussion

3 1. Influence of Matrix on the Long-Lifetime Triplet Excitons of Guest Molecules

$k_q(RT)$ encompasses the following four components: i) energy transfer from guest compounds to host matrix,[29,30] ii) diffusional motion of the matrix,[31–33] iii) concentration quenching of guest compounds, and iv) quenching by oxygen present in the host matrix.[34,35] Therefore, reduction of some or all of these four factors is required to decrease $k_q(RT)$. The $\tau(RT)$ of host-guest materials with metal complexes as the guest molecules and an organic matrix is not significantly affected by the diffusional motion of the matrix and oxygen present in the host matrix, because the k_r of metal complexes ($>10^4$ s^{-1})[8,9] is much larger than $k_q(RT)$ ($>10^2$ s^{-1}).[31,32] In contrast, the $\tau(RT)$ of pure organic host-guest materials, with conventional aromatic hydrocarbons as the guest molecules and an organic matrix, is strongly quenched because the k_r of the conventional aromatic hydrocarbons (around 10^0 s^{-1}) is much smaller than $k_q(RT)$ ($>10^2$ s^{-1}). This is because diffusional motion of the matrix and oxygen present in the host matrix results in the elimination of phosphorescence. To minimize $k_q(RT)$ considering the four components, an amorphous rigid structure with a large T_1 energy can be employed as the host matrix and this is a key factor in the host-guest design. In this study, β-estradiol (a hydroxyl steroidal compound), and a mixture of cholesterol (a hydroxyl steroidal compound) and the α,α,α′-*tris*(4-hydroxyphenyl)-1-ethyl-4-isopropylbenzene (THEB) [a phenol derivative] as shown in Figure 3b were investigated as the amorphous rigid host with a large T_1 energy. Other amorphous hosts in Figure 3b were used as a reference. In the following four paragraphs, the advantages of a hydroxyl steroidal compound as the host matrix for efficient persistent RTP were investigated using dye 9 and β-estradiol as the guest and host species, respectively. The structure of the dye 9 is shown in Figure 3a.

3.1.1. Influence of Endothermic Triplet-Triplet Energy Transfer from Guest Molecules to Steroidal Host

Energy transfer from dye 9 to the steroidal host in the material was not critical for depopulation of the triplet excitons of dye 9 at RT because of large T_1 energy of steroidal hosts. The spectral characteristics of β-estradiol and dye 9 are shown in (i)-(iii) and (iv)-(vi) of **Figure 4**a, respectively. Although (iii) and (iv) of Figure 4a represent that the T_1 state of dye 9 (2.4 eV) is much lower than that of β-estradiol (2.8 eV), long lifetime triplet excitons of dye 9 were quenched by endothermic triplet-triplet (T-T) energy transfer.[35] Figure 4b shows the temperature dependence of $k_{nr}(T)$+$k_q(T)$ when dye 9 was used as a guest in the β-estradiol host. The plots shown in Figure 4b can be expressed by the sum of two Arrhenius equations. $k_{nr}(T)$ contributes to the behavior observed at lower temperatures (blue line, Figure 4b), while that at temperatures above 240 K can be ascribed to the contribution of $k_q(T)$ (red line, Figure 4b). In the same manner,

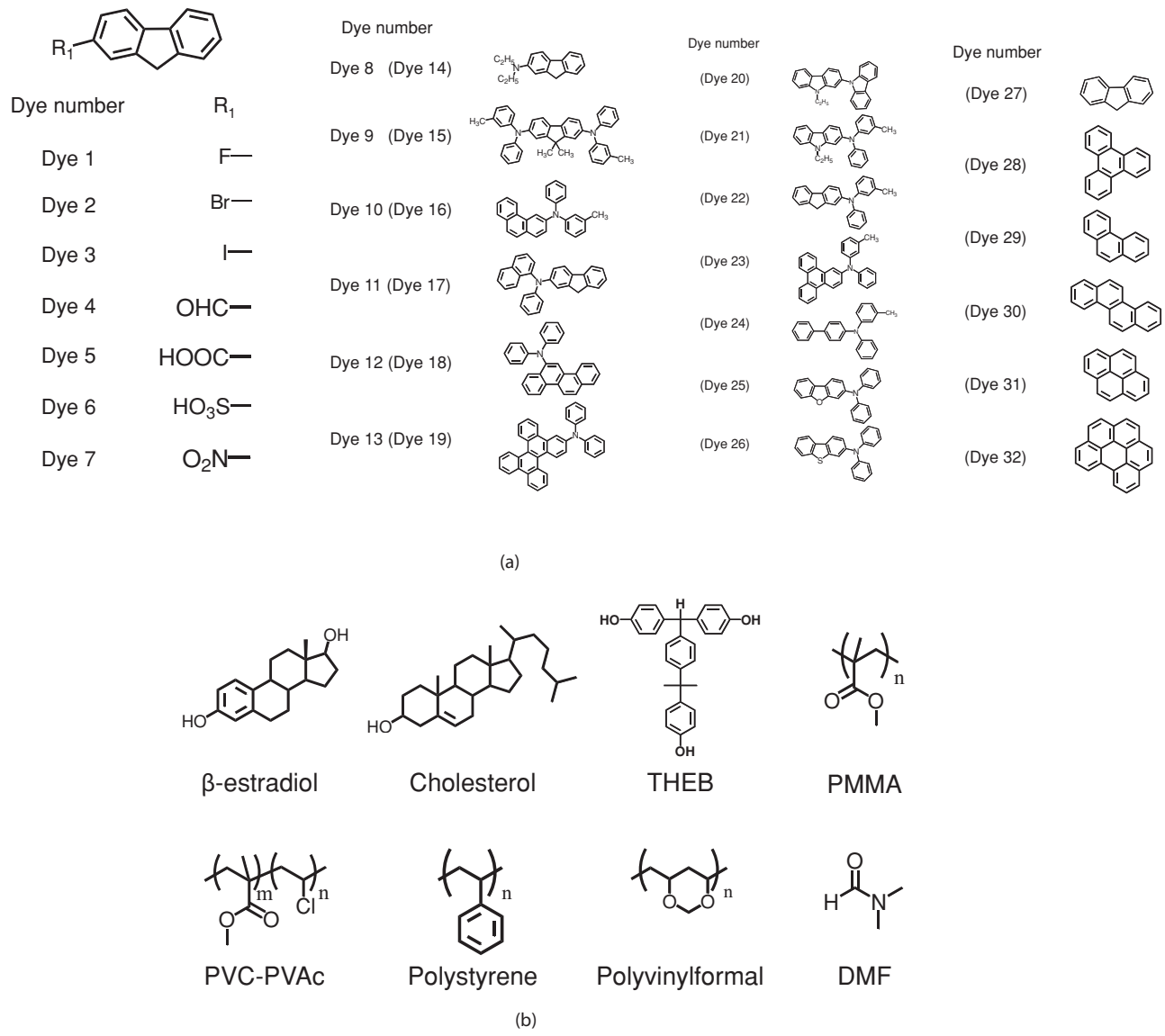

Figure 3. Molecular structures of the compounds used in this study. a) Structures of the guest compounds. Guest compounds with numbers in parentheses are deuterated dyes. b) Structures of the host compounds.

$k_q(T)$ was separated from $k_{nr}(T)+k_q(T)$ when various aromatic carbons were used as a guest in the β-estradiol host as shown in Figure 4c. The values of k_q(T) as shown in Figures 4b,c are caused by the endothermic T-T energy transfer from the guest to β-estradiol because the activation energies determined from Arrhenius plots of $k_q(T)$ vs (ΔG) for various aromatic carbon guest species in the β-estradiol host are proportional to the T_1 energy in the guests, and ΔG approaches 0 when the T_1 energy of a guest is close to that of β-estradiol (Figure 4d). However, $k_q(RT)$ in the guest species with visible phosphorescence is smaller than 3×10^{-1} s^{-1} as shown in Figure 4c. Since the values of $k_q(RT)$ is not so large to reduce triplet lifetime below 1 s based on Equation 2, the endothermic T-T energy transfer does not become a critical factor in a quenching of persistent RTP of guest species.

3.1.2. Influence of Diffusional Motion in Host Matrix

Diffusional motion in the steroid ring and alkyl side group of the amorphous steroidal compounds is suppressed below RT, which leads to a small $k_q(T)$ value over this temperature range when they were used as a host matrix. Therefore, the $\Phi_P(T)$ and $\tau(T)$ of dye 9 is not significantly decreased below RT (i.e., below the glass transition temperature (T_g)) under vacuum, when dye 9 was dispersed in the amorphous steroidal host matrices such as β-estradiol or a mixture of cholesterol and THEB ((B) and (A), respectively, in **Figures 5**a,b).

In contrast, a large decrease in the $\Phi_P(T)$ and $\tau(T)$ of dye 9 occurred at temperatures below RT under vacuum when a mixture of dimethylformamide (DMF) and a conventional polymer poly(methyl methacrylate) (PMMA) were used as the host

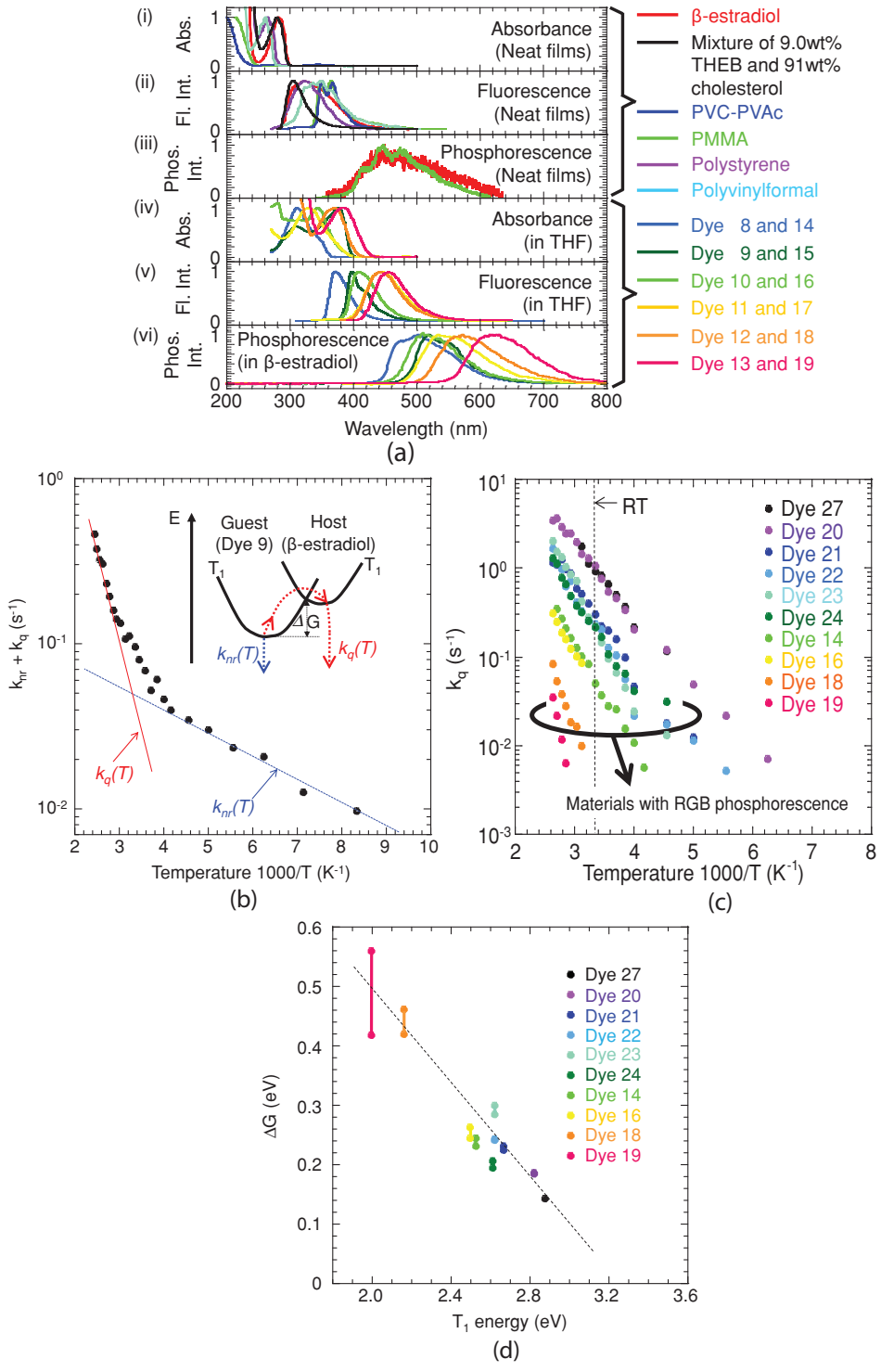

Figure 4. Investigation of the quenching of long-lived triplet excitons by endothermic triplet-triplet (T-T) energy transfer. a) Optical spectra of various host and guest compounds at RT ((i), (ii), (iv)-(vi)) and 5 K ((iii)). In (iii), phosphorescence was not observed at 5 K when mixture of THEB and cholesterol, poly(methylmethacrylate-vinylchloride) (PVC-PVAc), polystyrene, and polyvinylformal was used as an amorphous host matrix. In (iv)-(vi), spectral characteristics did not change between non-deuterated guests and deuterated ones. b) Rate constant of the nonradiative deactivation pathway ($k_{nr}(T) + k_q(T)$) as a function of temperature for the material composed of dye 9 (mass fraction 0.3%) and β-estradiol (mass fraction 99.7%). The inset shows that the nonradiative deactivation pathway in this material is ascribed to the nonradiative deactivation of dye 9 ($k_{nr}(T)$, blue arrow) and the endothermic T-T energy transfer from dye 9 to β-estradiol ($k_q(T)$, red arrow). Thin blue and red lines indicate fitting curves of $k_{nr}(T)$ and $k_q(T)$, respectively, based on the Arrhenius equation. After the endothermic T-T energy transfer, the triplet exciton of β-estradiol is deactivated to the ground state of β-estradiol. c, Temperature dependence of $k_q(T)$ in various combinations between a guest and β-estradiol. d) Activation energy of the endothermic T-T energy transfer from the guest to β-estradiol (ΔG) as function of the T_1 energy of the guest. In (c) and (d) a phosphorescent guest (mass fraction 0.3%) was dispersed in β-estradiol.

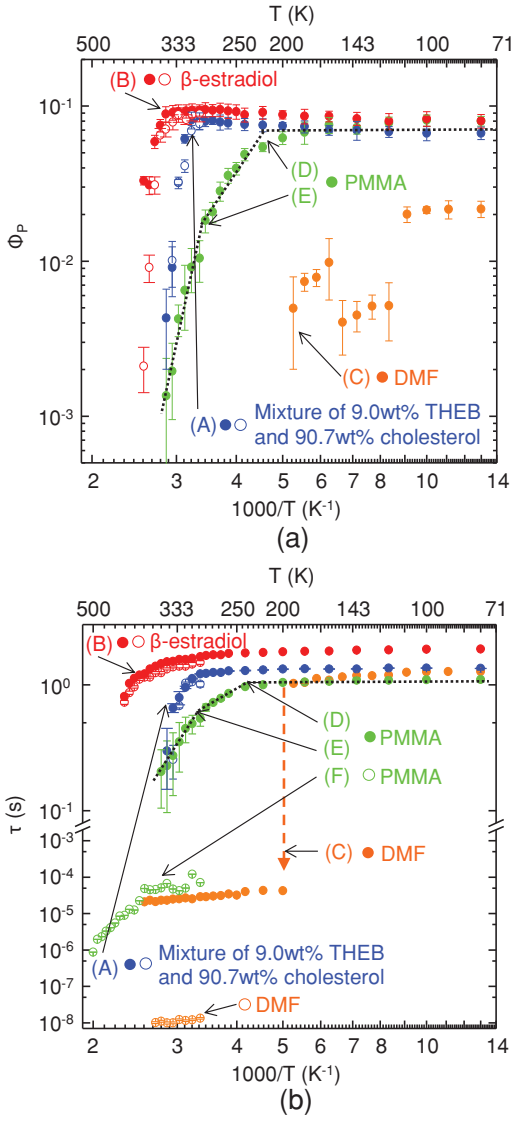

Figure 5. Quenching of the triplet excitons of dye 9 by thermal diffusional motion of the host. Dye 9 (mass fraction 0.3%) was dispersed in various matrices. a) Temperature dependence of $\Phi_P(T)$. The decrease in $\Phi_P(T)$ from 120–150 K can be ascribed to aggregation quenching of dye 9 induced by crystallization of the DMF matrix. b) Temperature dependence of $\tau(T)$. In a and b, open and solid symbols represent data under atmospheric conditions and vacuum, respectively. Black dotted lines are used to highlight the temperature dependence of $\Phi_P(T)$ and $\tau(T)$ for dye 9 dispersed in a PMMA matrix, respectively.

matrix. The active diffusion motion of DMF above its melting point (212 K) quenched long-lifetime triplet excitons at less than 100 μs ((C) in Figures 5a,b), resulting in complete elimination of phosphorescence. It is well-established that the emergence of diffusional motion, such as β- and α'-transitions in solid state matrix, quenches long-lifetime triplet excitons of guest molecules such as benzophenone.[31,32] Although T_g = 383 K[32] for PMMA is higher than T_g = 353 K (supporting information, Figure S7(ii)) for β-estradiol, a large decrease in $\Phi_P(T)$ and $\tau(T)$ of dye 9 in a PMMA matrix was observed with increasing temperature above 240 K under vacuum ((D) in Figures 5a and b). Nonexponential decay of phosphorescence for dye 9 was observed above 240 K when PMMA was used as the matrix (Supporting Information, Figure S9B), which indicates that β-relaxation of the side chain rotation in PMMA quenches long-lifetime triplet excitons of dye 9.[31,32] The change of the gradient of the solid green plots around 300 K in Figure 5a indicates that α'-relaxation of PMMA caused by local mode relaxation of the main CH_2 chain[32] also contributes to strong exciton quenching ((E) in Figures 5a and b).

Although we used other kinds of amorphous rigid hosts with no alkyl group such as polyimide and π conjugated polymers, persistent RTP of dye 9 was significantly quenched. This is because significant endothermic T-T energy transfer from dye 9 to the hosts occurs since T_1 energy of the hosts is not so large compared to that of dye 9 and it completely hides a contribution of diffusional motion of host to the quenching of triplet exciton of dye 9. Therefore, steroidal compound is one of host matrices with both rigid characteristics due to cyclo ring structure and high T_1 energy due to short π conjugation, and it could be an appropriate candidate for host matrix with $k_q(T)$.

3.1.3. Influence of Aggregation of Guest Molecules

It has been reported that steroidal host matrix with hydroxyl group forms thermally stable amorphous states at RT,[36] which provides easy dispersion of incorporated guest molecules. The good dispersion suppresses concentration quenching of the guest molecules, which leads to efficient persistent RTP when appropriate chemical structure was used as a guest. For example, a steroidal host matrix composed of cholesterol (mass fraction 90.7%) and THEB (mass fraction 9.0%) shows amorphous state at RT, which is confirmed by X-ray and polarization optical microscope (POM) measurements (Supporting Information, Figures S7(i) and S8A, respectively). Dye 9 dispersed in the mixture matrix showed persistent RTP but it was quenched due to active diffusional motion of the steroidal host matrix when the host-guest film was heated to the temperature between T_g = 313 K and the crystallization temperature (T_c = 333 K) ((A) in **Figure 6**a(ii)). However, the quenched phosphorescence intensity of dye 9 was recovered when it was cooled to below T_g again ((B) in Figure 6a(ii)). This is because dye 9 was not aggregated due to no crystallization of the steroidal host in the heat cycle. In contrast, the phosphorescence intensity of dye 9 was not recovered when the host-guest film was crystallized at 363 K for 1 min. ((C) in Figure 6a(iii)) and then cooled to below T_g ((D) in Figure 6a(iii)).[37] This is because the crystallization of the host matrix induces aggregation of dye 9, leading to strong concentration quenching of dye 9. In the same manner, a host-guest film composed of dye 9 and β-estradiol showed the persistent phosphorescence below T_g = 353 K of β-estradiol as shown in red symbols of Figures 5a,b because dye 9 is dispersed in β-estradiol due to amorphous state of β-estradiol host at the temperature range.[38] However, persistent phosphorescence of dye 9 was not recovered due to aggregation of dye 9 induced by crystallization of β-estradiol when it was cooled to RT after long time heating of β-estradiol at 403 K.[39]

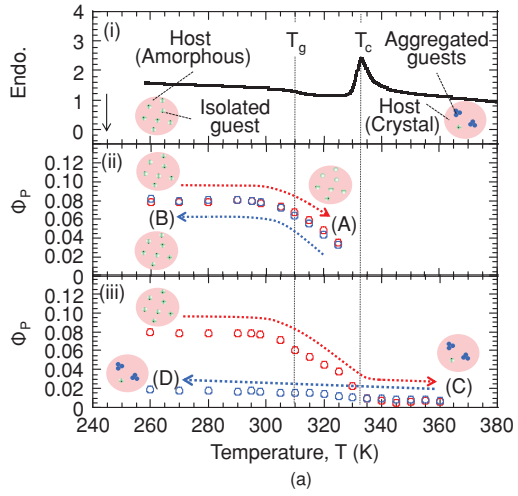

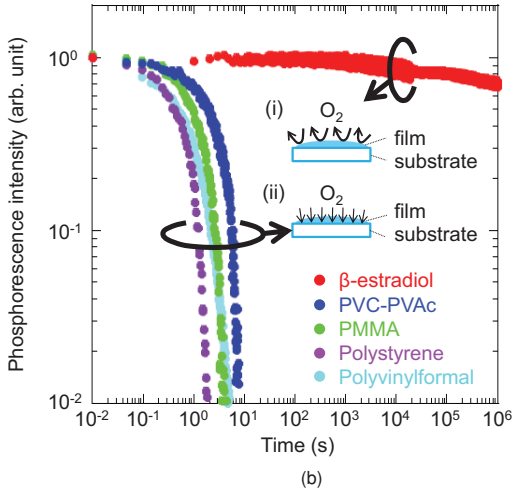

Figure 6. Quenching of the triplet excitons of dye 9 by aggregation of the guest and oxygen quenching. a) Differential scanning calorimetry (DSC) and phosphorescence characteristics of a host-guest material composed of dye 9 (mass fraction 0.3%), THEB (mass fraction 9.0%) and cholesterol (mass fraction 90.7%) during heat treatment. The host-guest material was prepared by a quenching from the temperature of melting point to RT. (i) DSC characteristics when the host-guest material is heated from 260 K. (ii) RTP intensity changes during heating of the host-guest film from 260-325 K, annealing at 325 K for 1 min, and then cooling to 260 K. (iii) RTP intensity during heating from 260-360 K, annealing at 325 K for 1 min, and then cooling to 260 K. Temperature was changed at a scan rate of 5 K min^{-1}. In (ii) and (iii), red and blue symbols represent heating and cooling processes, respectively. b) Phosphorescence intensity of the samples under vacuum when exposed to an excitation source after injection of air. The air was injected at 0 s. Inset (i) shows that oxygen does not diffuse into the host-guest film containing the β-estradiol host matrix, and inset (ii) represents oxygen diffusion into conventional host matrix.

3.1.4. Influence of Oxygen Diffusion

Oxygen in steroidal compounds is naturally degassed in air by heating to a temperature higher than the melting point (M_P) (Supporting Information, Section 3), and a significant low concentration of oxygen is preserved for a long time, because of the slow diffusion of oxygen into steroidal compounds. This preserves the long-lifetime RT triplet excitons of the guest species. Comparison of some of the plots in Figure 5b (i.e., open and solid red and blue symbols; most of these are overlapped at a low temperature) indicates that the persistent phosphorescence of dye 9 is not significantly quenched by oxygen when β-estradiol or a mixture composed of cholesterol and THEB is used as an amorphous steroidal host, respectively.[40] This can be ascribed to significant small diffusion coefficient of oxygen into the steroidal matrix because RTP did not decrease after injection of oxygen from vacuum condition in case of β-estradiol (red symbols, Figure 6b). In contrast, comparison of other plots in Figure 5b (i.e., open and solid green symbols) indicates that the long-lifetime triplet excitons of dye 9 are quenched by oxygen in less than a millisecond in air when a conventional amorphous polymer such as PMMA is used as the matrix ((F) in Figure 5b). This is because of the large diffusion coefficient of oxygen into conventional host matrix because RTP quickly decrease after injection of oxygen from vacuum condition (purple, sky blue, green, and blue symbols, Figure 6b).

All the quenching factors based on interactions between the guest and host matrix or oxygen could be reduced by using an amorphous rigid steroidal compound as the host matrix. The $k_q(RT)$ was less than 10^{-1} s^{-1} when dye 9 and β-estradiol were used as the guest species, respectively. This is because $k_{nr}(T)+k_q(T)$ is less than 10^{-1} s^{-1} below RT in that case (Figure 4b). We note that the value of $k_q(RT)$ is significant small compared to that in other conventional organic amorphous hosts.

3.2. Optimum Structure of Guest Molecules for Efficient Persistent RTP.

For organic persistent RTP, it is important to identify pure organic guest molecules with small $k_{nr}(RT)$ in steroidal host. The $k_{nr}(RT)$ values of pure organic guest molecules with conventional host materials have not been experimentally measured in air, because the $k_q(RT)$ are large (>10^2 s^{-1}).[31,32] However, the $k_{nr}(RT)$ values can be measured in air when an amorphous steroidal compound is used as the host, because the $k_q(RT)$ are significantly small (<10^{-1} s^{-1}). Based on Equations 1 and 2, $k_{nr}(RT)$ should be smaller than k_r for both high $\Phi_P(RT)$ and long $\tau(RT)$. $k_{nr}(T)$ can be expressed by Equations 3 and 4 (Supporting Information, Section 1.3).[28,41–45]

$$k_{nr}(T) \propto f_S f_V \exp(-\Delta G'/kT) \quad (3)$$

$$f_V = \exp(-\alpha \Delta E/\hbar\omega) \quad (4)$$

where f_S and f_V represent the prohibition factors caused by changes in the spin configuration and the Franck-Condon factor, respectively; ΔE represents the maximum energy of phosphorescence; $\Delta G'$ is the activation energy of nonradiative processes from T_1 state; ω is the energy of an effective nonclassical vibrational mode involved in the nonradiative transition, which is typically determined by the highest frequency vibration mode, such as the C-H stretching vibration in aromatic guest molecules;[45] α is a constant; k is the Boltzmann constant. Control over decreasing ΔE is rather difficult to achieve,

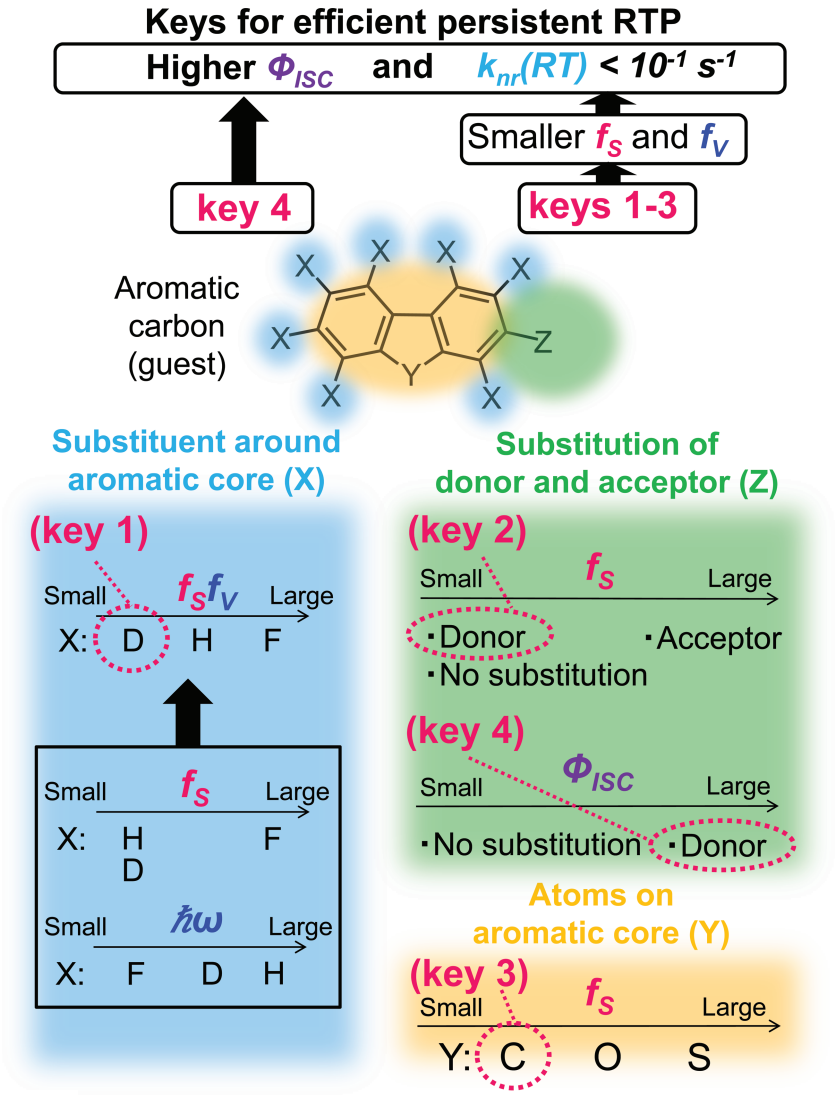

Figure 7. Molecular design of a guest compound for efficient persistent RTP. Efficient persistent RTP can be obtained by controlling molecular key elements (keys 1 to 4).

because ΔE is limited from 1.8 eV to 3.2 eV with RGB phosphorescence; however, f_S and $\hbar\omega$ can be controlled by changing the molecular structure of the guest compound. The decrease of f_S and $\hbar\omega$ is important because it leads to decrease $k_{nr}(T)$ based on Equations 3 and 4.

Figure 7 summarizes a design of the guest to decrease both f_S and $\hbar\omega$ for efficient persistent RTP; it is concluded that keys 1-3 in Figure 7 are necessary for smaller $k_{nr}(RT)$ and key 4 is also important to obtain higher $\Phi_{ISC}(RT)$ for efficient persistent RTP in air. **Figures 8**a–d and the following three paragraphs describe the rate constant of the nonradiative deactivation pathway ($k_{nr}(T)$+$k_q(T)$) for each guest molecule, which shows adequacy of the guest design shown in Figure 7.[46] In Figure 8a–d, each guest molecule with phosphorescence energy lower than 2.6 eV is doped into β-estradiol host. The value of $k_{nr}(T)$ in Figures 8a–d is the dominant component of the sum of $k_{nr}(T)$ and $k_q(T)$ below RT, because the value of $k_q(T)$ in host-guest film composed of the guest and β-estradiol host is less than 10^{-1} s^{-1} below RT as shown in Figure 4b, which is always smaller than $k_{nr}(T)$+$k_q(T)$ below RT shown in Figures 8a–d. From the result of $k_{nr}(T)$ at low temperature range in Figures 8a–c, we investigated the increase and decrease of f_V, f_S, ΔE, and $\Delta G'$ by introduction of deuteration, different substituent groups, and heavy atoms, respectively. This investigation indicates that a structural design as shown in Figure 7 is required for the guest with persistent RTP characteristics.

3.2.1. Reduction of Nonradiative Deactivation from T_1 State by Decreasing Franck-Condon Factor

The value of $\hbar\omega$ can be reduced by deuteration of the aromatic hydrocarbons without significant change of f_S, which leads to smaller $f_S f_V$ (key 1, Figure 7).[28],[45] Figure 8a shows that $k_{nr}(T)$ for the aromatic hydrocarbons containing secondary amine substituents can be decreased by deuteration over the whole temperature range. Similar slopes of $k_{nr}(T)$ vs $1/T$ below RT in Figure 8a indicate that $\Delta G'$ is almost the same in these compounds. Therefore, the decrease of $k_{nr}(T)$ is ascribed to a decrease of $f_S f_V$ based on Equation 3. Since f_S does not decrease by deuteration because the spin orbital coupling constant of D is not lower than that of H, the result of Figure 8a indicates that deuteration decreases f_V. Furthermore, the phosphorescence spectra of the guest compounds shown in Figure 8a did not change after deuteration, which indicates that the values of ΔE are the same for non-deuterated and deuterated guest compounds. Therefore, ω of deuterated aromatic carbons is smaller than that of non-deuterated ones based on Equation 4, which is a critical factor to determine a decrease of $k_{nr}(T)$ in Figure 8a. Although it was expected that fluorination around the aromatic core would reduce $\hbar\omega$ because vibrational energy of C-F stretching mode is smaller than that of C-D stretching mode, it also significantly increases f_S by heavy atom effect. Therefore, $f_S f_V$ of the fluorinated aromatic carbons is larger than that of non-fluorinated aromatic hydrocarbons, which results in the larger $k_{nr}(T)$ of the former (Supporting Information, Section 5).

3.2.2. Reduction of Nonradiative Deactivation from T_1 State Due to Weak Spin Orbit Coupling by Selection of Proper Substituent of Aromatic Carbons

It is suggested that the f_S values of aromatic hydrocarbons cannot be increased by the introduction of secondary amines substituents (key 2, Figure 7). The $k_{nr}(RT)$ values in secondary amino-substituted aromatic hydrocarbons (circles, Figure 8b) are around 10^{-1}-10^{0} s^{-1} at RT, and are 100 times smaller than those of fluorenes containing acceptor substituents (squares,

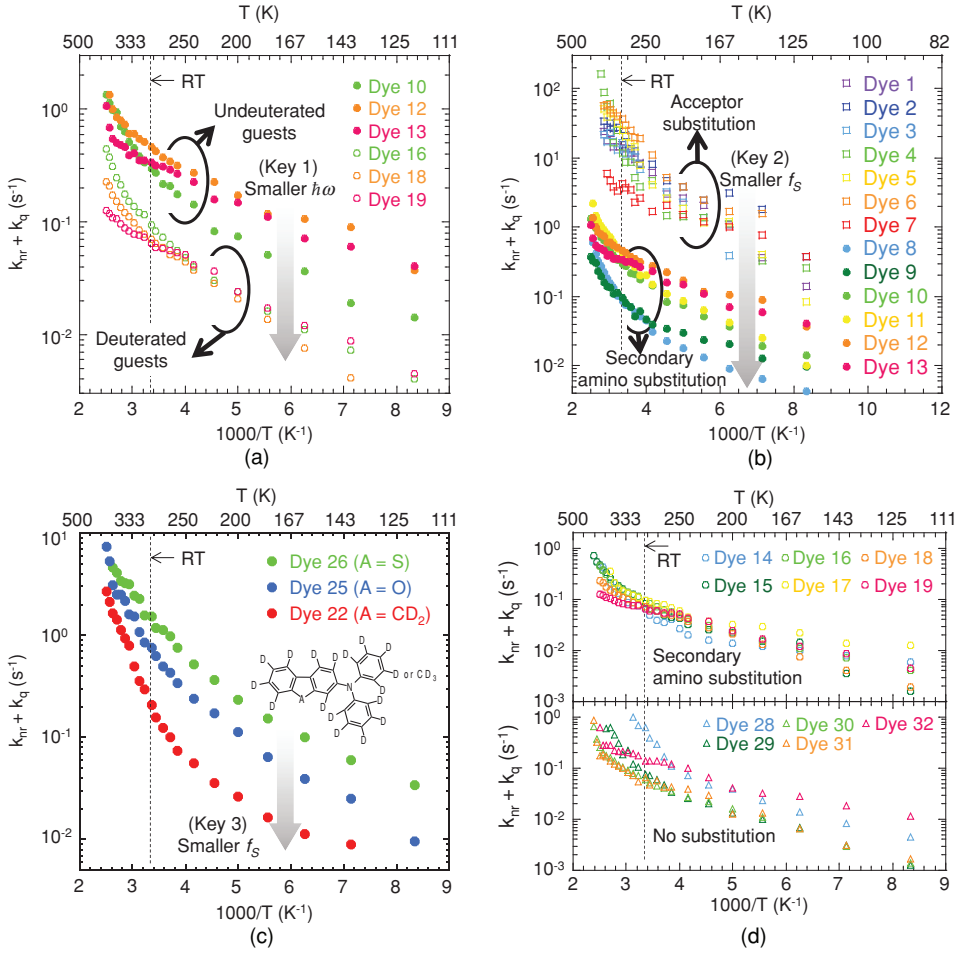

Figure 8. Temperature dependence of $k_{nr}(T)$ of host-guest films composed of the guest compounds (mass fraction 0.3%) and β-estradiol host. a) Difference in the sums of $k_{nr}(T)$ and $k_q(T)$ between aromatic hydrocarbons with secondary amino-substituents (solid circles) and deuterated aromatic hydrocarbons with secondary amino-substituents (open circles). b) Temperature dependence of the sum of $k_{nr}(T)$ and $k_q(T)$ in aromatic hydrocarbons with acceptor substituents (squares) and secondary amine substituents (circles). c) Influence of atomic weight in the aromatic core on the sum of $k_{nr}(T)$ and $k_q(T)$. d) Temperature dependence of the sum of $k_{nr}(T)$ and $k_q(T)$ for deuterated aromatic hydrocarbons with secondary amino-substituents (upper panel) and unsubstituted deuterated aromatic hydrocarbons (lower panel).

Figure 8b). The values of $\Delta G'$ are almost the same for the hydrocarbons containing secondary amines and acceptor substituents, as shown by the similar slopes of the plots in Figure 8b. In addition, it is suggested that the ω values are not significantly different between these compounds. This is because $\hbar\omega$ is determined mainly by the C-H bonds of aromatic cores[28,45] and the aromatic core of the guests shown in Figure 8b has the same structure such as a non-deuterated fluorene. Furthermore, ΔE does not change in these compounds (Supporting Information, Figures S23D and S24D). Based on Equation 4, the no significant changes of $\hbar\omega$ and ΔE between the donor substituted guests and the acceptor substituted ones leads to similar f_V among the guests. Therefore, it is suggested that the difference of $k_{nr}(T)$ can be ascribed to the difference of f_S based on Equation 3. It has been reported that the n-orbital of oxygen in the carbonyl group of substituted aromatic hydrocarbons is not parallel to the π-orbitals of the aromatic carbons, which relaxes spin forbidden processes.[28,44] Therefore, it is probable that electrons anti-parallel to the π-orbitals of the aromatic carbons in the acceptor group substituents increase f_S, which will increase $k_{nr}(T)$.

3.2.3. Reduction of Nonradiative Deactivation from T_1 State Due to Weak Spin Orbit Coupling by use of Light Atoms in Aromatic Carbons

The use of a lightweight atom at a location near the aromatic core reduces the f_S factor (key 3, Figure 7). In Figure 8c, the nonradiative processes of dyes 22, 25, and 26 dispersed in a β-estradiol host matrix were evaluated. The three guests have the same aromatic structure and the only difference is the atom at the 9 position of the aromatic core; $k_{nr}(T)$ increases with the atomic weight of the atom at the 9 position. $\Delta G'$ is almost the same in the three guests, as indicated by the similar

slopes of $k_{nr}(T)$ vs $1/T$. Furthermore, in the three guests, ΔE is similar because they have the same aromatic structure (Supporting Information, Figure S25(iii)). $\hbar\omega$ cannot be increased with an increase of the atomic weight at the 9 position in the three guests because the introduction of the heavier atom decreases an energy of stretching vibration. Therefore, f_V is not increased based on Equation 4 with an increase of the atomic weight. Since Figure 8c represents that $f_S f_V$ increases with the atomic weight at the 9 position of the three guests, the increase of $k_{nr}(T)$ in Figure 8c is ascribed to f_S. Therefore, the difference of $k_{nr}(T)$ in Figure 8c is ascribed to f_S. Although atoms such as O, F, and S are not recognized as heavy atoms, the slight increase of f_S should be eliminated by employing lighter atoms in the aromatic core to produce long-lifetime RT triplet excitons.

3.3. Efficient Persistent RTP Characteristics in Air

The minimization of both f_S and f_V for deuterated aromatic carbons with secondary amino-substituents in a β-estradiol matrix provides $k_{nr}(T)<10^{-1}$ s^{-1} below RT (Figure 8d, circles). Although the values of k_r in these guest compounds are below 10^0 s^{-1} as shown in **Figure 9**a, $k_{nr}(T)+k_q(T)$ are smaller than k_r below RT. Consequently $\tau(T)$ and $\Phi_P(T)$ do not significantly change from 77 K to RT, based on Equations 1 and 2 (Figures 9a,b).

In addition, the substituted aromatic carbons (Figure 9b, circles) have higher $\Phi_P(T)$ than the unsubstituted aromatic carbons (Figure 9b, triangles) from 77 K to RT. On the other hand, the $k_{nr}(T)$ values of the deuterated aromatic carbons with secondary amino-substituents (Figure 8d, circles) are almost the same as those of the unsubstituted deuterated aromatic carbons (Figure 8d, triangles) from 77 K to RT. These results indicate that the $\Phi_{ISC}(RT)$ values of the aromatic hydrocarbons with secondary amino-substituents are higher than those of the unsubstituted deuterated aromatic carbons based on Equation 1 (key 4, Figure 7).

Consequently, both the large $\Phi_{ISC}(RT)$ and minimization of $k_{nr}(RT)+k_q(RT)$ ($<10^{-1}$ s^{-1}) resulting from material design (Figure 1(i)) using a combination of appropriate guest design (Figure 7) and an amorphous steroidal host resulted in efficient persistent RTP with a quantum efficiency of >10% (Figure 9b) and a lifetime >1 s (Figure 9a). Persistent RTP spectra were observed at longer wavelengths relative to the fluorescence spectra under continuous excitation (**Figure 10**a, upper). After photoexcitation was stopped, only the persistent RTP components were observed for several seconds (Figure 10a, lower) with single exponential decay characteristics (Figure 10b).

In this proposed organic persistent RTP materials, $k_{nr}(T)$ and $k_q(T)$ are significantly suppressed because the values of Φ_P and τ hardly increase with a decrease of temperature from RT to 5 K. Therefore, an increase of $\Phi_{ISC}(RT)$ is a key to increase $\Phi_P(RT)$. The use of heavy atom in guest compound is not good approach because it leads to a decrease of $\tau(RT)$ that loses persistent RT emitting characteristics. Therefore, we suggest that efficient triplet-triplet energy transfer from sensitizer with high $\Phi_{ISC}(RT)$ to the aromatic deuterated carbons as shown in this research will make possible of organic persistent RTP materials with larger $\Phi_P(RT)$.

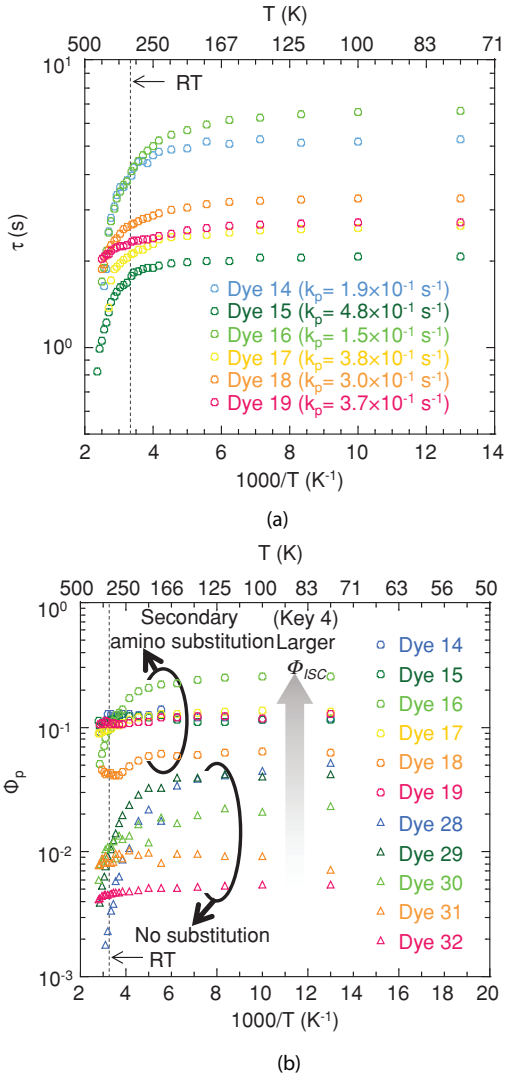

Figure 9. Temperature dependence of $\tau(T)$ and $\Phi_P(T)$. a) $\tau(T)$. b) $\Phi_P(T)$. Host-guest films composed of the guest compounds (mass fraction 0.3%) and β-estradiol host.

4. Conclusions

Efficient persistent RGB RTP was achieved from pure organic amorphous host-guest materials in air. The use of amorphous rigid steroidal compounds as a host matrix significantly minimizes quenching of long-lifetime RT triplet excitons of the guest species by interaction with the host matrix and oxygen. Deuteration of the guest reduces its nonradiative decay rate. Furthermore, substitution of the aromatic guest with a secondary amino-group does not increase the nonradiative decay rate of the guest, but enhances intersystem crossing from the S_1 state to T_1 state. Consequently, the host-guest systems provide both a nonradiative deactivation pathway from the T_1 state at less than 10^{-1} s^{-1} at RT and effective intersystem crossing from the S_1 state to T_1 state. This allows for efficient persistent RGB RTP with a quantum yield >10% and a lifetime >1 s in air. The pure organic amorphous host-guest materials are nontoxic and

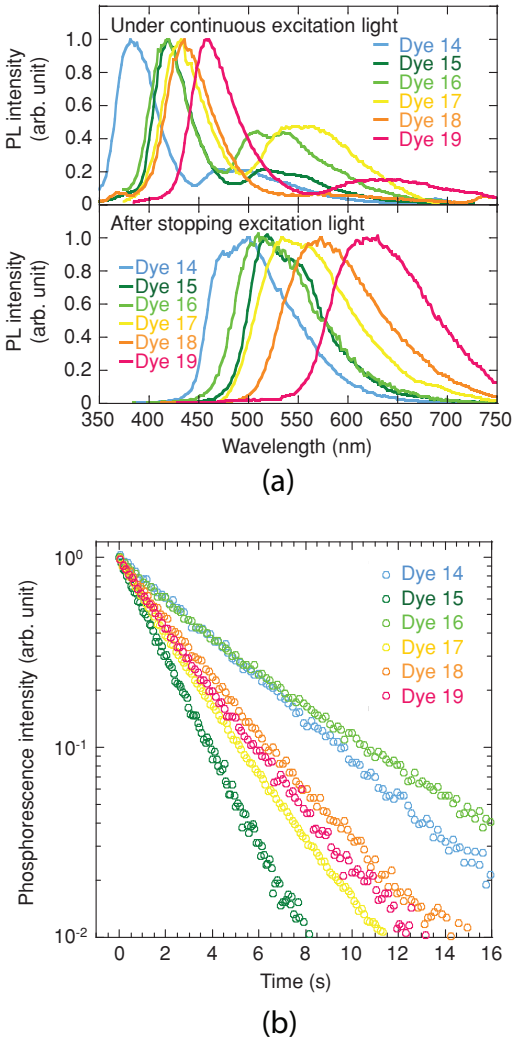

Figure 10. Spectra and lifetime characteristics of RTP in host-guest films composed of the guest compounds (mass fraction 0.3%) and β-estradiol host. a) Photoluminescence spectra under continuous excitation (top) and RTP spectra taken 5 s after stopping photoexcitation (bottom). b) Phosphorescence decay characteristics at RT in air.

abundant, and would be useful for background-independent imaging applications. Thus, identification of appropriate materials design to achieve efficient persistent RTP in air could be significantly important for the next generation imaging technology and display applications.

5. Experimental Section

Synthesis: Dyes 9–12 and 14–26 were synthesized by the methods shown in the Supporting Information, Section 1.1. The dyes were deuterated by treating the undeuterated dye (100 mg) with Pd (mass fraction 10%) on activated carbon (75 mg, 0.1 mmol Pd) and D_2O (15 g) in a 30 mL teflon-lined autoclave at 240°C for 12 h. The internal pressure reached 4–5 MPa. Ethyl acetate (100 mL) was added after slowly cooling to RT. The D_2O phase of the reaction was washed three times with ethyl acetate (50 mL each time). After filtration through silica gel, the filtrate was dried over Na_2SO_4 and then filtered. Evaporation of the solvent yielded the crude deuterated product. The crude material was purified by column chromatography to give the target compound (Details provided in supporting information, section 1.1). All other compounds used were commercially available.

Film preparation: Samples were prepared using a steroidal compound as the matrix and addition of a guest compound (mass fraction 0.3%) to the host material. The mixture was heated on a hotplate to a temperature higher than M_P of the host material, which dissolved the guest compound into the melted host material. This mixture was dropped onto a glass substrate that was also heated on a hotplate to M_P of the host material. The glass plate was then cooled to RT. The entire procedure was conducted in air. Samples were prepared using a conventional polymer as the matrix; a polymer film containing the guest compound (mass fraction 0.3%) was fabricated on a glass substrate by spin casting a solution of DMF containing dye 9 (mass fraction 0.06%) and polymer (mass fraction 10%) at 1000 rpm for 60 s at 333 K. All procedures were conducted in air.

Physical Properties of the Steroid Matrix: X-ray diffraction patterns of the steroid matrix and mixtures of steroidal compounds and phenol derivatives were measured using a Rigaku RAD-C diffractometer. A Rigaku Thermo Plus DSC8230 instrument and an Olympus BX50 microscope were used for DSC and POM measurements, respectively.

Temperature Dependence of the Quantum Yield, Fluorescence and Phosphorescence Lifetimes: UV-vis and fluorescence spectra were measured on Jasco V560 and FP-6500 spectrometers, respectively. The fluorescence quantum yield at RT ($\Phi_F(RT)$), $\Phi_P(RT)$, and $\tau(RT)$ of the host-guest films were measured using an integrating sphere (FIS415, Jasco) equipped with a time-resolved charge-coupled device (MCPD-7000, Otsuka Electronics) and an excitation unit attached to the spectrophotometer (FP-6500, Jasco). The temperature of each sample was increased from 5–430 K using a temperature controller attached to a cryostat (Oxford Ltd. Optistat DN-V) to investigate the temperature dependence of the fluorescence intensity, phosphorescence intensity, and phosphorescence lifetime. The $\Phi_F(T)$ and $\Phi_P(T)$ values of host-guest films composed of a dye dispersed in various matrices were calculated using the change in the ratio of fluorescence (or phosphorescence) intensity at a set temperature (K) to fluorescence (or phosphorescence) intensity at RT. Details are given in Section 1.2 of the Supporting Information.

Determination of k_r, $k_{nr}(T)$, and $k_q(T)$: Nonradiative decay of guest molecules in the T_1 state does not occur at 5 K ($k_{nr}(5\ K) + k_q(5\ K) = 0$), because the phosphorescence lifetime of the guest compounds does not change around 5 K. Therefore, k_r was calculated using $k_r = 1/\tau(5\ K)$ based on Equation 1. The total values of $k_{nr}(T)$ and $k_q(T)$ at each temperature can be calculated using $k_{nr}(T) + k_q(T) = 1/\tau(T) - k_r$, which is based on Equation 2.

Supporting Information

Supporting Information is available from the Wiley Online Library or from the author.

Acknowledgements

S. H. designed the materials and S. H. and J. Z. synthesized the compounds. S. H. performed the deuteration experiments. S. H., K. T., and T. Y. measured the photophysical characteristics, collected the data, and performed the analyses. S. H., K. T., S. M., H. K., T. W., and C. A. drafted the manuscript. All authors discussed the progress of research and reviewed the manuscript. This research was supported by International training program to Pre-Tenure-Track Young Researchers in "Nano-Materials" at the Tokyo University of Agriculture and Technology supported by the Japan Society for the Promotion of Science (JSPS) International Training Program (ITP), a Grant-in-Aid for Young Scientists (B) (22750132), Adaptable and Seamless Technology Transfer

Program through Target-driven R&D (AS231Z01236B), Grant-in-Aid for Challenging Exploratory Research (24655175), a Grant-in-aid from the Funding Program for World-Leading Innovative R&D on Science and Technology (FIRST). This article was modified after online publication. Prof. T. Watanabe was designated as a corresponding author.

Received: December 14, 2012
Published online: February 6, 2013

[1] W. L. Rumsey, J. M. Vanderkooi, D. F. Wilson, *Science* **1998**, *241*, 1649.
[2] J. G. J. E. D. Dolmans, D. Fukumura, R. K. Jain, *Nat. Rev. Cancer* **2003**, *3*, 380.
[3] H. A. Collins, M. Khurana, E. H. Moriyama, A. Mariampillai, E. Dahlstedt, M. Balaz, M. K. Kuimova, M. Drobizhev, V. X. Yang, D. Phillips, A. Rebane, B. C. Wilson, H. L. Anderson, *Nat. Photonics* **2008**, *2*, 420.
[4] J. W. Perry, K. Mansour, S. R. Marder, K. J. Perry, D. Alvarez, I. Choong, *Opt. Lett.* **1994**, *19*, 625.
[5] G. J. Zhou, W. Y. Wong, S. Y. Poon, C. Ye, Z. Lin, *Adv. Funct. Mater.* **2009**, *19*, 531.
[6] M. A. Baldo, D. F. O'Brien, Y. You, A. Shoustikov, S. Sibley, M. E. Thompson, S. R. Forrest, *Nature* **1998**, *395*, 151.
[7] C. Adachi, M. A. Baldo, M. E. Thompson, S. R. Forrest, *J. Appl. Phys.* **2001**, *90*, 5048.
[8] L. Flamigni, A. Barbieri, C. Sabatini, B. Ventura, F. Barigelletti, *Top. Curr. Chem.* **2007**, *281*, 143.
[9] A. J. Gareth Williams, *Top. Curr. Chem.* **2007**, *281*, 205.
[10] G. Zhang, G. M. Palmer, M. W. Dewhirts, C. L. Fraser, *Nat. Mater.* **2009**, *8*, 747.
[11] S. Zhang, M. Hosaka, T. Yoshihara, K. Negishi, Y. Iida, S. Tobita, T. Takeuchi, *Cancer Res.* **2010**, *70*, 4490.
[12] W. Z. Yuan, X. Y. Shen, H. Zhao, J. W. Y. Lam, L. Tang, P. Lu, C. Wang, Y. Liu, Z. Wang, Q. Zheng, J. Z. Sun, Y. Ma, B. Z. Tang, *J. Phys. Chem. C* **2010**, *114*, 6090.
[13] O. Bolton, K. Lee, H. J. Kim, K. Y. Lin, J. Kim, *Nat. Chem.* **2011**, *3*, 205.
[14] Q. I. M. de Chermont, C. Chaneac, J. Seguin, F. Pelle, S. Maitrejean, J. P. Jolivet, D. Gourier, M. Bessodes, D. Scherman, *Proc. Natl. Acad. Sci. USA* **2007**, *104*, 9266.
[15] P. Zhengwei, L. Yi-Ying, L. Feng, *Nat. Mater.* **2012**, *11*, 58.
[16] H. W. Leverenz, *Science* **1949**, *109*, 183.
[17] K. V. den Eeckhout, P. F. Smet, D. Poelman, *Materials* **2010**, *3*, 2536.
[18] M. Irie, T. Fukaminato, T. Sasaki, N. Tamai, T. Kawai, *Nature* **2002**, *420*, 759.
[19] Y. C. Liang, A. S. Dvornikov, P. M. Rentzepis, *Proc. Natl. Acad. Sci. USA* **2003**, *100*, 8109.
[20] R. Ando, H. Mizuno, A. Miyawaki, *Science* **2004**, *306*, 1370.
[21] A. Kishimura, T. Yamashita, K. Yamaguchi, T. Aida, *Nat. Mater.* **2005**, *4*, 546.
[22] T. Mutai, H. Satou, K. Araki, *Nat. Mater.* **2005**, *4*, 685.
[23] S. Hirata, T. Watanabe, *Adv. Mater.* **2006**, *18*, 2725.
[24] S. Hirata, K. S. Lee, T. Watanabe, *Adv. Funct. Mater.* **2008**, *18*, 2869.
[25] T. Fukaminato, T. Doi, N. Tamaoki, K. Okuno, Y. Ishibashi, H. Miyasaka, M. Irie, *J. Am. Chem. Soc.* **2011**, *133*, 4984.
[26] S. Habuchi, R. Ando, P. Dedecker, W. Verheijen, H. Mizuno, A. Miyawaki, J. Hofkens, *Proc. Natl. Acad. Sci. USA* **2005**, *102*, 9551.
[27] P. Dedecker, J. -I. Hotta, C. Flors, M. Sliwa, H. Uji-i, M. B. J. Roeffaers, R. Ando, M. Mizuno, A. Miyawaki, J. Hofkens, *J. Am. Chem. Soc.* **2007**, *129*, 16132.
[28] S. K. Lower, M. A. El-sayed, *Chem. Rev.* **1966**, *66*, 199.
[29] J. N. Turro, *Modern Molecular Photochemistry*, University Science Books, Sausalito, California **1991**, pp. 331–338.
[30] C. Adachi, M. A. Baldo, S. R. Forrest, S. Lamansky, M. E. Thompson, R. C. Kwong, *Appl. Phys. Lett.* **2001**, *79*, 2082.
[31] K. Horie, I. Mita, *Chem. Phys. Lett.* **1982**, *93*, 61.
[32] K. Horie, K. Morishita, I. Mita, *Macromolecules* **1984**, *17*, 1746.
[33] K. Horie, H. Ando, I. Mita, *Macromolecules* **1987**, *20*, 54.
[34] J. Kuijt, F. Ariese, U. A. Brinkman, C. Gooijer, *Anal. Chem. Acta* **2003**, *488*, 135.
[35] P. F. Jones, S. Siegel, *J. Chem. Phys.* **1969**, *50*, 1134.
[36] K. Naito, *Appl. Phys. Lett.* **1995**, *67*, 211.
[37] DSC and POM in Supporting Information Figure S7(i) and X-ray data in Figure 8B indicate crystallization of the sample by annealing for 1 min at 360 K.
[38] DSC and POM in Supporting Information Figure S7(ii) and X-ray data in Figure 8C indicate amorphous state the sample at RT.
[39] DSC and POM in Supporting Information Figure S7(ii) and X-ray data in Figure 8D indicate crystallization of the sample by annealing for 1 min at 403 K.
[40] Temperature dependence of $\Phi_P(T)$ and $\tau(T)$ did not show significant difference between in air and in vacuum when other aromatic compound and β-estradiol were used as a guest and an amorphous steroidal host, respectively.
[41] J. N. Turro, *Modern Molecular Photochemistry*, University Science Books, Sausalito, California **1991**, pp. 153–198.
[42] K. Schmidt, S. Brovelli, V. Coropceanu, D. Baljonne, J. Cornil, C. Bazzini, T. Caronna, R. Tubino, F. Meinardi, Z. Shuai, J-L. Bredas, *J. Phys. Chem. A* **2007**, *111*, 10490.
[43] W. Siebrand, *J. Chem. Phys.* **1967**, *46*, 440.
[44] G. W. Robinson, R. P. Frosch, *J. Chem. Phys.* **1963**, *38*, 1187.
[45] M. Gouterman, *J. Chem. Phys.* **1962**, *36*, 2846.
[46] Data of Figure 8 were calculated using phosphorescence characteristics shown in Figures S12-S22 of the Supporting Information.